

## Microseismicity Induced by Heavy Rainfall Around Flooded Vertical Ore Veins

HIROSHI OGASAWARA,<sup>1</sup> KUNIO FUJIMORI,<sup>2</sup> NAOJI KOIZUMI,<sup>3</sup> NORIO HIRANO,<sup>4</sup>  
SATOSHI FUJIWARA,<sup>5</sup> SHIGEAKI OTSUKA,<sup>6</sup> SETSURO NAKAO,<sup>4</sup> KIN'YA NISHIGAMI,<sup>7</sup>  
KEISUKE TANIGUCHI,<sup>8</sup> YOSHIHISA IIO,<sup>9</sup> RYOHEI NISHIDA,<sup>10</sup>  
KAZUO OIKE,<sup>2</sup> and YUTAKA TANAKA<sup>2</sup>

*Abstract*—Microseismicity ( $M < 0$ ) induced by heavy rainfall was investigated around the flooded, vertically dipping Tertiary ore veins with dimensions of about  $1 \text{ km} \times 1 \text{ km}$  in the Ikuno mine, Japan. The ore veins had rock bursts ( $M < 3$ ) before the mine was closed in 1973, as well as seismic events ( $M < 3$ ) during flooding after it was closed down. The stress state is therefore critical to failure, at least within one stress drop of a seismic event. Since 1987, when the veins had become mostly flooded, 56 mine tremors ( $M < 0$ ) were observed over a 5-year period. Several times during this five-year period the mine sustained heavy rainfall of several tens of millimeters per day, and the water table flooding over the ore veins was elevated by several meters. Significant changes in strain larger than  $10^{-6}$  were also monitored at a crustal movement monitoring station located several hundred meters from the veins. It was found that the opening of the vertical ore veins primary led to significant strain and tilt, but not to seismicity, because the delay and the longer duration of the seismicity were significant. Most seismic events involve thrusting mechanisms that are consistent with the present stress state of E-W-oriented tectonic compression, but are not consistent with the opening of the deepest ore vein. Interestingly, all the events within a few months of the heavy rainfall occurred near the faults that offset the deepest ore veins, whereas all those events located away from the deepest ore veins occurred many months after the heavy rainfall. Consequently, the delayed diffusion of water appears to have played a dominant role in reducing rock strength, which led to seismicity in the Ikuno mine.

<sup>1</sup> Faculty of Science and Engineering, Ritsumeikan University, 1-1-1 Noji Higashi, Kusatsu, 525-8577, Japan. E-mail: ogasawar@se.ritsumei.ac.jp

<sup>2</sup> Graduate School of Science, Kyoto University, Sakyo-ku, Kyoto, 606-8502, Japan.

<sup>3</sup> Geological Survey of Japan, 1-1-3, Higashi, Tsukuba, Ibaraki, 305-8567, Japan.

<sup>4</sup> Research Center of Earthquake Prediction, Disaster Prevention Research Institute, Kyoto University, Gokasho, Uji, 611-0011, Japan.

<sup>5</sup> Geographical Survey Institute, 1 Kitasato, Tsukuba, 305-0811, Japan.

<sup>6</sup> Faculty of Humanities and Sciences, Kobe Gakuin University, 518 Arise, Ikawadani-cho, Nishi-ku, Kobe, 651-2180, Japan.

<sup>7</sup> Research Center for Disaster Reduction Systems, Disaster Prevention Research Institute, Kyoto University, Gokasho, Uji, Kyoto 611-0011, Japan.

<sup>8</sup> Kyoto University of Education, 1 Fukakusa-Fujinomori-cho, Fushimi-ku, Kyoto, 612-8522, Japan.

<sup>9</sup> Earthquake Research Institute, the University of Tokyo, 1-1-1 Yayoi Bunkyo Tokyo 113-0032, Japan.

<sup>10</sup> Department of Civil Engineering, Faculty of Engineering, Tottori University, 4-101, Koyama-Minami, Tottori, 680-8552, Japan.

**Key words:** Seismicity, flooded mine, deep vein, faults, heavy rain, multidisciplinary monitoring.

### 1. Introduction

Induced or triggered earthquakes may be caused by changes in stress and/or pore pressure, as reviewed in MCGARR and SIMPSON (1997). We discuss the contribution of each type of change, using available data.

One of the earliest examples of seismicity caused by fluid injection occurred in Colorado ( $M < 5$ ) at a pressure on the order of 10 MPa (EVANS, 1996; HEALY *et al.*, 1968). The seismicity was both simultaneous and delayed with respect to the injection. It was later found that an increase in pore pressure of 1 to 5 MPa was enough to trigger the seismicity (FLETCHER and SYKES, 1977).

The impoundment of water by huge reservoirs also contributes to significant seismicity (RALEIGH *et al.*, 1976). However, once a critical state of stress has been established by impounding the water, much smaller fluctuations of water than those involved in injection experiments have sometimes simulated the seismicity. For example, SIMPSON and NEGAMATULLAEV (1981) found that a drop in water level of a few meters (on the order of 0.01 MPa) and a rapid decrease in the reservoir-filling rate (0.5 m/day) stimulated seismicity. SIMPSON *et al.* (1988) showed that reservoir-triggered seismicity can be divided into two types – a rapid reaction related to instantaneous elastic response, and a delayed reaction related to fluid diffusion.

The studies noted above have mainly been concerned with seismicity, and with descriptions of tectonic settings and the magnitude of water pressure. The stress state in seismic source areas has been inferred in some studies however mostly this has been based on numerical estimation (SIMPSON and NEGAMATULLAEV, 1981). Few studies have tried to infer stress states in source areas using *in situ* strain and tilt data.

A deep, flooded mine can be regarded as a huge water reservoir in which the enclosing rocks have generally been well investigated. The Ikuno mine is one of the deepest flooded mines in Japan with vertically dipping ore veins. It was closed down in 1973 because of severe rock bursts (maximum  $M = 2.4$ ; TANAKA and NISHIDA, 1971, 1977; NISHIDA and TANAKA, 1972), and flooding subsequent to the closure induced seismicity (maximum  $M = 2.9$ ; TANAKA and NISHIDA, 1977; TANAKA and OKA, 1979). The increase in water level was closely monitored, and it was shown that there was a good correlation between water level and seismicity. Unfortunately, only one seismometer with a rotating-drum recording system was installed in the mine. This seismometer counted events with small S-P times, and more detailed measurements were not taken. A similar case history in flood-induced seismicity in a hard rock mine in Canada (WETMILLER *et al.*, 1993) yielded seismograms like multiplets, suggesting similar mechanisms during flooding stages. However, reliable water-level data were few and there were no seismic stations in the mine.

By 1976 the Ikuno mine was mostly flooded. Ikuno sometimes experiences heavy rainfall amounting to several tens of millimeters per day, with the resulting water table elevated by several meters. The Ikuno mine has an underground crustal movement monitoring station on intact rock, so that *in situ* strain and tilt data are available. In addition, we deployed a small underground seismic array on intact rock within the mine to detect seismicity. In this paper we present a case study of seismicity involving a deep, flooded, vertical ore vein, and discuss the relationship between the seismicity and heavy rainfall.

## 2. *Ikuno Mine with Flooded Vertical Veins and a History of Induced Seismicity*

The Ikuno mine is adjacent to an area of naturally high seismicity in southwestern Japan, as shown in Fig. 1(a), and minor active faults (RESEARCH GROUP for ACTIVE FAULT, 1990) have been studied near the Ikuno mine (Fig. 1(b)). However, very few natural earthquakes ( $M > 1$ ) have been measured in the years 1965–1984 by the microearthquake monitoring network of Kyoto University in an area of several km<sup>2</sup> immediately surrounding the Ikuno mine, (Fig. 1(b)).

The ore veins in the Ikuno mine originated from Tertiary hydrothermal activity. Most ore veins were intruded nearly vertically into Tertiary volcanics overlying Paleozoic sedimentary rocks (Fig. 2).

The fault system in Ikuno is characterized by NE-SW-striking, nearly vertical faults (the Nendo and Sanjugo faults), as well as by conjugate NW-SE-striking faults dipping northeast (the Nii and Juichii faults). As noted in Table 1, the former faults are relatively significant and their associated fissure zones are well developed, resulting in a NE-SW-striking valley about 10 km long (Figs. 2 and 3). The latter faults are relatively minor, but also have significant lateral offset (the Senjuhon-hi vein is right-laterally offset by the Nii fault in Fig. 2 (upper)). The activity of these faults began after the intrusion of the ore veins and therefore the ore veins have clear offsets as shown in Table 1, consistent with the Tertiary N-S compressive tectonic stress. Although the present principal tectonic stress state is E-W compression (TANAKA *et al.*, 1989), these faults are still oriented to cause seismic events.

The Ikuno mine has a long history that began in 806 A.D., more than a thousand years ago. Numerous small tunnels, called ‘raccoon dog’s holes,’ were excavated by chisel and hammer in the early historic period. By the late 1960s, the excavation had reached a depth of about 1 km in the Kanagase area. The Kinsei-hi vein, Senju-hon-hi vein and Senju-zen-hi vein were the deepest and were excavated to a depth of about 1 km (~500 m altitude in Figs. 2 and 3). The largest rock bursts of about  $M = 2$  occurred at the Kinsei-hi and Senjuhon-hi veins from 1970 to 1972 (Figs. 2 and 4); TANAKA and NISHIDA, 1971; NISHIDA and TANAKA, 1972), and were measured and located by the microearthquake monitoring network of the Disaster Prevention Research Institute of Kyoto University (Fig. 1(c)). These rock bursts

forced closure of the Ikuno mine in 1973, as noted. The drain pumps at the deepest level of the mine were stopped, and the excavation began to flood. The total amount of water flooding the mine by the late 1970s was in excess of several tens of millions of tons. TANAKA and NISHIDA (1977) and TANAKA and OKA (1979) installed a

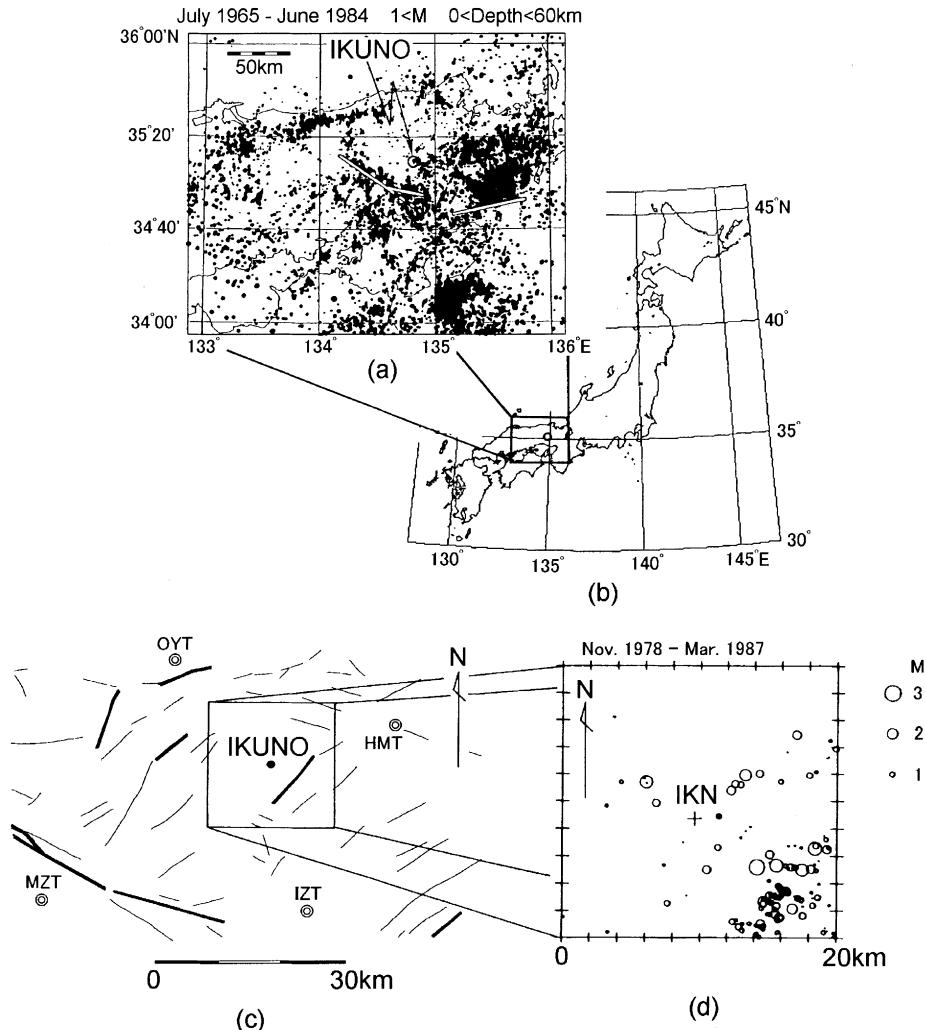


Figure 1

Location of the Ikuno mine, background seismicity and active faults. (a and b) Location of the Ikuno mine and regional seismicity around the mine. (c) Active faults (thick lines) and lineaments (thin lines). Microseismic monitoring stations of the Disaster Prevention Research Institute, Kyoto University are shown by double circles. (d) Enlarged view of the distribution of microearthquakes around the Ikuno mine. (The microseismicity data from the Disaster Prevention Research Institute, Kyoto University; fault data from the Research Group for Active Faults, 1990).

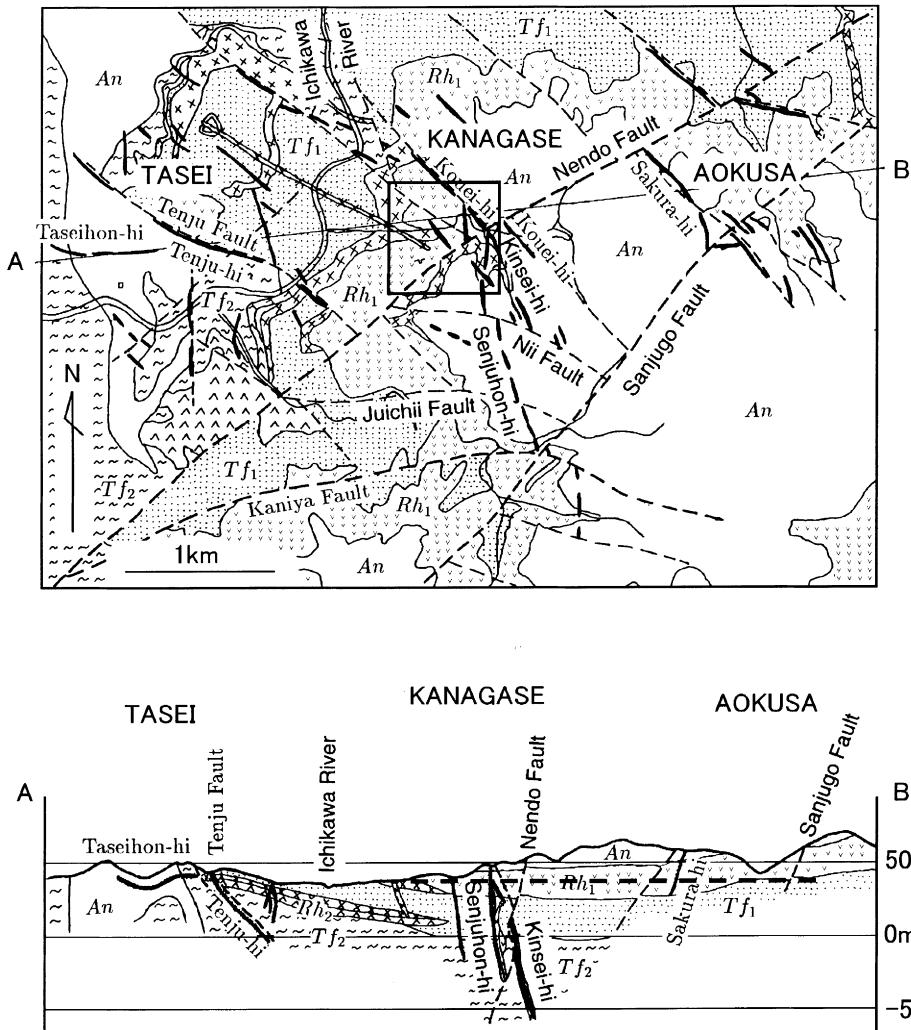


Figure 2

Geology of the Ikuno mine. Upper: plan view, lower: cross section. An, Rh and Tf: andesite, rhyolitic welded tuff and tuff, respectively. The Ikuno mine consists of three areas: Tasei, Kanagase, and Aokusa. The Kanagase area has the deepest ore veins. Note that ore veins are offset significantly by the Nendo, Nii and Sanjugo faults. The 750 m × 750 m square in the Kanagase area in the upper figure shows where we installed instruments (see Fig. 3). A horizontal dashed line in the lower figure represents an underground level where a geophone array is deployed and a crustal movement monitoring station is located.

seismometer with a rotating-drum recording system and counted the events with short S-P times. While the mine was being flooded, these instruments detected the water-induced earthquakes, the maximum magnitude being about three (Fig. 4). More-detailed seismicity was not investigated at the time, however. By 1976, most of

Table 1  
Major faults in the Kanagase area, Ikuno mine

Fault	Strike	Dip	Lateral offset (m)	Thrust offset (m)
Nendo	NE-SW	85	100 (left)	40
Sanjugo	NE-SW	85	170 (left)	10
Nii	NW-SE	68	70 (right)	20
Juichii	NW-SE	67	40 (right)	10

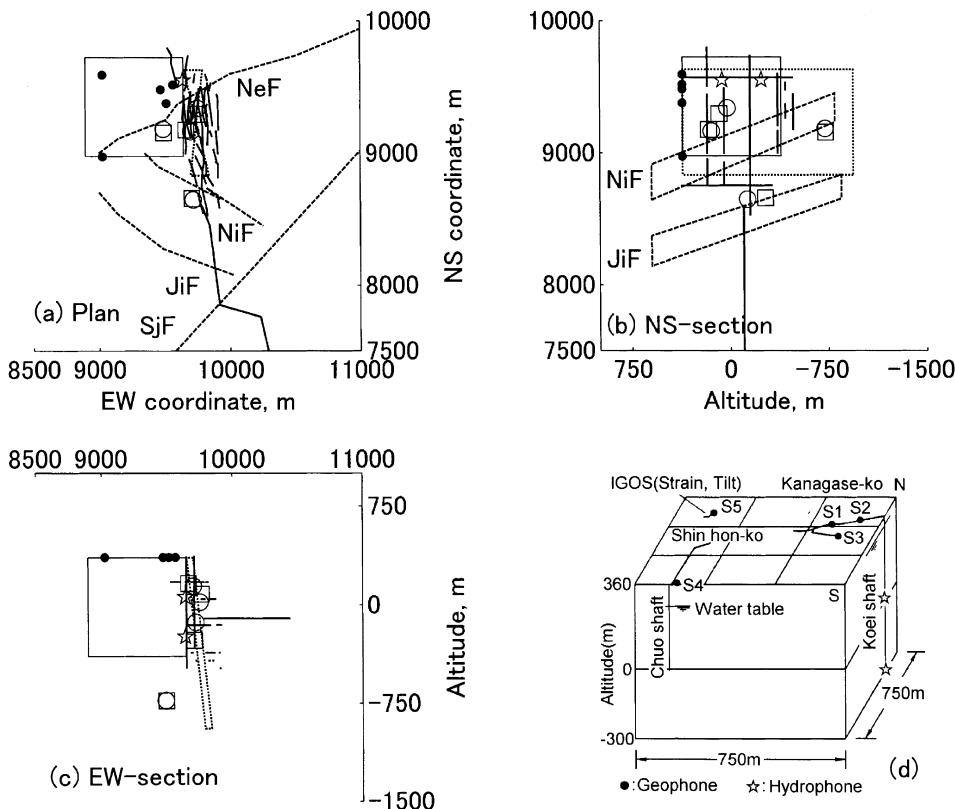


Figure 3

Configuration of faults, flooded tunnels and instruments around the ore veins. Faults are shown by dashed lines in (a) and (b). NeF: Nendo fault, NiF: Nii fault, JiF: Juichii fault, SjF: Sanjugo fault. Flooded tunnels at the deep, mined ore veins are shown by thick, solid lines in (a), (b) and (c). The dotted rectangle in (a), (b) and (c) is the location of the hypothesized tabular cavity discussed in the text as the source of the observed changes in strain and tilt. A 750 m × 750 m square in (a), (b) and (c) represents a cubic area where we installed the instruments shown in (d). Geophones and hydrophones are shown by dots and stars, respectively. Circles and small squares show the location of four events determined by both geophones and hydrophones, and by geophones only, respectively. Extensometers and tiltmeters are installed at the Ikuno Geophysical Observation Station (IGOS). The level of water flooding the mined ore veins was measured in the Koei shaft.

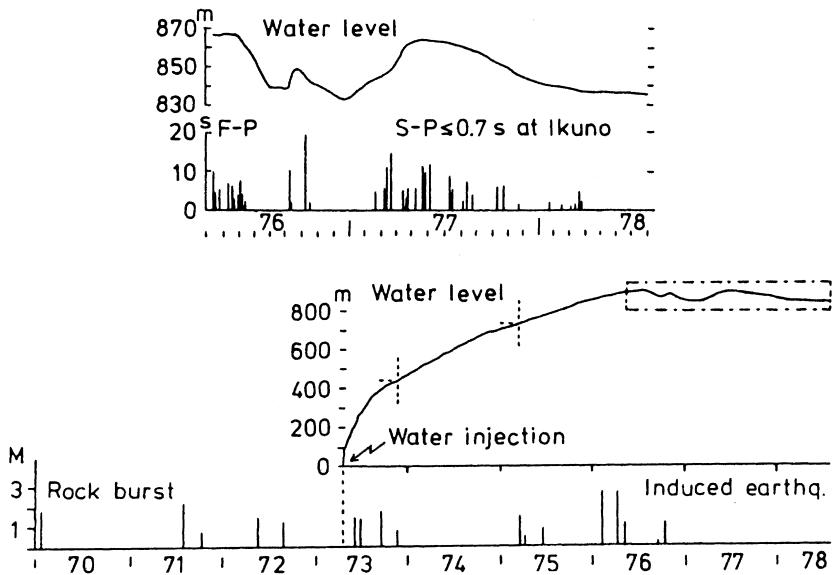


Figure 4

Water table elevations and induced earthquakes from 1970 to 1978 (after TANAKA and OKA, 1979). (Lower): The water level above the bottom of the excavation and the magnitude of rock bursts and earthquakes. (Upper): Enlarged. The Ikuno mine was closed down in 1973 and experienced large induced earthquakes after most of it flooded by 1976; from 1977 on, seismicity was associated with a rise in the water table from approximately 835 m to some 860 m.

the excavated area was flooded. To prevent the leakage of polluted water from a number of 'raccoon dog's holes', drain pumps were installed and began to lower the water table to about 50 m below the level of the Ichikawa River (Fig. 2), the seismicity then decreased.

### *3. Rainfall and the Underground Water System*

The level of the underground water that floods all the deeply excavated cavities in the Kanagase area (Figs. 2 and 3) is measured at the Koei shaft (Fig. 3(d)) by an engineer with a measuring device once a day. Water is then drained by pumps in this shaft, if the water level is relatively high. The drain pumps operate for several days, hence we can see variations in the water level with an amplitude of a few meters and making plots that look like saw teeth when it rains slightly (Fig. 5(f)). Since the Ikuno mine has open pits as well as numerous historic 'raccoon dog's holes', rainfall can easily flow into the excavated cavities. Heavy rainfall of several tens of millimeters per day (Fig. 5(c)) has sometimes caused rapid elevation of the water level (Fig. 5(e)) that the pumps could not reduce. The resulting elevation of the water level has been as high as several meters (Fig. 5(f)).

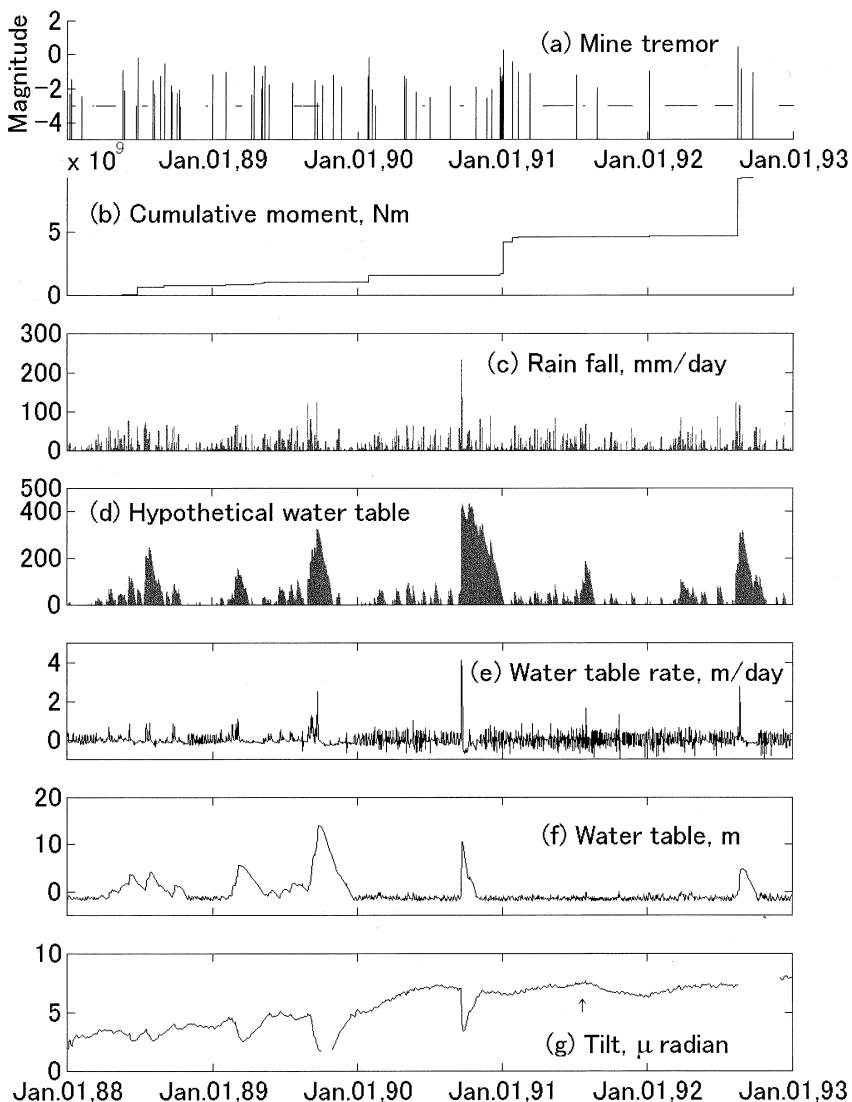


Figure 5

Relationship between Seismicity (a), cumulative seismic moment (b), rainfall (c), underground water table (f) and tilt (g) for five years starting in 1988. Synthetic water level is shown in (d) for comparison, obtained by assuming the accumulation of rainfall and a constant drainage rate best-fit to the observed water table fluctuation until 1990, just before the drain pumps were replaced by more efficient ones. Rate of water table rise is calculated from (f) and is also shown in (e). Note the immediate, significant response of the tilt to the water level, and the slow, small response of the tilt to the large cumulative rainfall (d) in the middle of 1991 (shown by an arrow), which continued for several months.

To understand how the water table responded to rainfall, we compared the observed water table (Fig. 5(f)) with a hypothetical water table (Fig. 5(d)). To obtain the hypothetical water table (Fig. 5(f)), we first subtract the pumps' effects from the cumulative rainfall, assuming that the pumps are operating only during positive cumulative rainfalls. A constant rate of pump drainage was assumed, in order to get a best-fit of the hypothetical water table up to 1990. As seen in Fig. 5(d), the hypothetical water table matches the observed water level very well until the end of 1989. Therefore, we can regard the water system that floods the ore veins basically as a huge reservoir with input from rainfall and output by pumping. The pumps were replaced by more efficient ones in 1990, so the subsequently observed water level (Fig. 5(f)) has been relatively low, compared with the hypothetical water table (Fig. 5(d)). There was no significant elevation of water level in the middle of 1991, despite rainfall as significant as in 1989, owing to the more efficient pumps.

#### 4. Strain and Tilt, and its Relation to the Water System

##### a) Observations and Data

The Ikuno Geophysical Observation Station (hereinafter IGOS; Fig. 3(d)), which monitors crustal movement, is several hundred meters to the WNW of the flooded vertical ore veins, and in hard rock (rhyolitic welded tuff) with an overburden of hard rock about 40 m thick. In IGOS, four extensometers (EXT) with super-Invar pipes 5–10 m long, and water tube tiltmeters (WTT) with four pots at intervals of 10 m, are installed in a redundant configuration to reliably monitor the strain and tilt field most. Four horizontal pendulum-type tiltmeters (HPT) are also in operation however we have used their records only to check the sense of tilt observed by the WTTs, because the HPTs tend to be significantly affected by local effects. Strain and tilt have been monitored with resolution sufficient for detecting earth tides as small as  $10^{-8}$  (Tabei *et al.*, 1985) and calibrated well with theoretical earth tides (Koyama, 1988).

##### b) Elastic Response to Water Level

Figure 5(g) shows tilting in the N28W–S28E direction. Comparing Figure 5(g) with Figure 5(f), it is clear that the tilt correlates well to fluctuations of the water table. Also note the tilt in the middle of 1991 (an arrow in Fig. 5(g)); a significant increase is seen in the hypothetical water table (Fig. 5(d)), while no *prima facie* changes are seen in either the water table or the tilt. Thus the tilt always responds to the water level, although not always to the hypothetical water level. Because the water table reflects water pressure, elastic response to the increase in water pressure can account well for such changes in tilt. Since a similar correlation with the water table can be seen in strain, the elastic response can also account well for the change in strain.

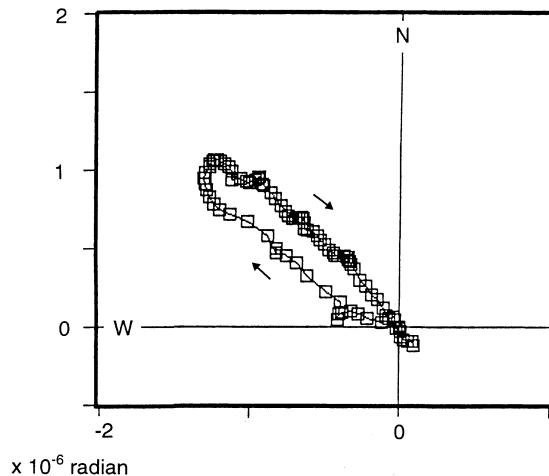


Figure 6

Typical example of tilt response to significant elevation of the water level (from February 16 to May 16, 1989). The direction of maximum tilt and the magnitude of the tilt are represented by a vector from origin to square plotted for each day. Immediately after the rainfall of May 16 a tilt began toward the northwest with an increase in the water level, and a reversal of the tilt with a decrease of the water level. Since the deep ore veins are located southeast of IGOS, uplift is required at the ore veins to account for the observed tilt.

Figure 6 shows a typical example of the tilt response to a significant elevation of water level for about four months in 1989. It rained 81 mm in three days starting February 16, and 238 mm in ten days starting February 24, consequently the water level was elevated about 6 m higher than usual. The ground tilted down to the northwest along with the elevation of the water table, and recovered as the water table lowered.

Strain changes associated with the rainfall in February 1989 are shown in Table 2. The sense of strain is different in different directions, suggesting that significant shear strain occurred in association with the rainfall.

As shown in Table 2, subsidence measures by water weight will lead to tilt or extension in a southeast direction, because the ore veins are located to the southeast of IGOS. Therefore, the weight of water cannot account for the tilt and strain.

Here we will consider if the opening of a vertical tabular cavity in the deepest ore veins can account for the observed strain and tilt, because rainfall will increase water pressure and the associated opening will produce vertical deformation on the surface, as shown in Figure 7. The strain and tilt were estimated by dislocation theory and computer code by OKADA (1992). The widest tabular cavity (1300 m deep, 800 m long and 1300 m wide) that covers all areas of the deepest veins and hypocenters was initially used for estimation, as denoted by a dotted square in Figures 3(a–c). By changing the depth of the upper edge of the tabular cavity, we tried to find the best-case solution. The best-case solution thus obtained is shown in the rightmost columns

in Table 2. Because the correlation coefficient is 0.86, we conclude that a cavity with its upper edge at an altitude of 210 m and an opening of 1.6 cm is the best model accountable for the observed strain and tilt.

Table 2

*The observed strain and tilt ( $\times 10^{-6}$ ) and comparison with the synthesized ones. One of the assumed tabular cavities (1300 m deep, 800 m long and 1300 m wide; upper edge at a depth of 360 m) is shown in Figure 3 by a dotted line*

	Observed	Subsidence model	Cavity opening model		
			Opening Upper edge	0.39 cm 360 m	1.4 cm 110 m
Tilt (W down)	1.4	-		0.22	0.26
Tilt (N down)	1.1	-		0.24	0.91
Strain (N28W)	-0.3	+		-0.8	-0.33
Strain (N73W)	-0.3	+		-0.09	-0.02
Strain (N17E)	0.42	-		-0.12	0.9
Correlation coefficient =				0.52	0.86

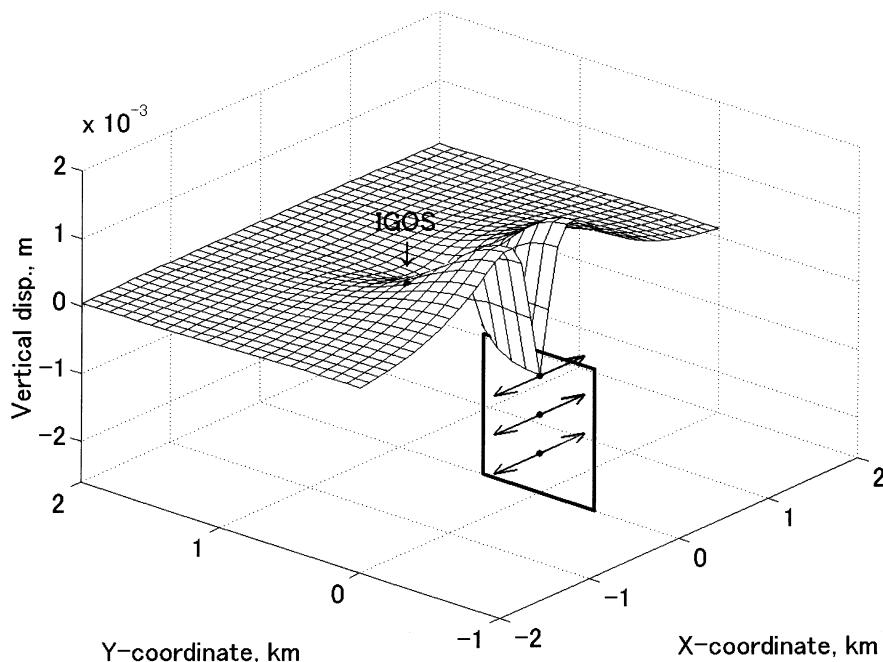


Figure 7

Schematics showing a model that accounts for uplift in the direction of the ore veins. If we assume that a vertical tabular cavity opens, and that IGOS is located as shown in this figure, then uplift in the direction of the ore veins is observed at IGOS.

### *c) Slow and Delayed Response to Rainfall*

If we attend more to tilt in the middle of 1991 (an arrow in Fig. 5(g)) however, there was a gradual change in tilt that steadily decreased by about  $2 \times 10^{-6}$  until the end of 1991 and recovered in April 1992. We also noted such changes starting after heavy rainfalls and continuing for several months. Therefore, we think that the diffusion of underground water may be responsible for these changes. Most cavities made by mining had already been filled with sand or slime, and the mine has faults with high permeabilities. Consequently, poroelastic response associated with the diffusion of water may be responsible for the gradual change and recovery.

## *5. Seismic Events Associated with Heavy Rainfall*

### *a) Monitoring and Location of Mine Tremors*

Seismic events in the mine have been monitored since 1987 using geophones at five sites, and temporary hydrophones in the flooded Koei shaft (Figs. 3(d); OGASAWARA *et al.*, 1992) using a PC recording system with a 12-bit, 2-kHz sampling A/D board. All geophones (Mark Products L22-D) were installed on intact rock (rhyolitic welded tuff) in haulage tunnels at the 360-m altitude level (shown by a dashed line in Fig. 2 (lower)) with an overburden of intact rock of from a few tens to a hundred meters. Before installing geophones we struck the rock with a hammer to carefully ascertain that it was neither floated nor fissured. All geophones were glued to the rock with cement. A 3-component geophone was installed at site S3 and only vertical components at other sites. As shown in Figure 8, events with magnitudes as low as  $-2.5$  were clearly detected by the system. Events that simultaneously triggered at least three geophone sites were recorded and used for analysis. Hydrophones were not used as a trigger source, so there was no difference in the trigger threshold of the recording system whether the hydrophones were in operation or not.

Errors in  $P$ -reads were within a few ms.  $S$ -reads at site S3 and other available sites were used for hypocenter locations.  $V_p = 4.65$  km/s was determined by blasting at a quarry about 1 km to the west of our seismic array. A homogeneous isotropic elastic medium and  $V_s = V_p/\sqrt{3}$  was assumed for the hypocenter location. A hydrophone at a deeper level in the Koei shaft (at an altitude of  $-300$  m; Fig. 3) was in operation for only a month from the end of December 1987, and the shallower one for a considerably shorter period. However, one event was recorded by 2 hydrophones and 4 geophones, and three more events were recorded by a deeper hydrophone and 5 geophones. Using these records we determined station corrections to minimize residuals. The maximum station correction was about 10 ms for  $P$ -reads for geophone sites within ore veins. Corrections for hydrophones were plus or minus 5 ms, being independent of depth. The locations of the four events determined with

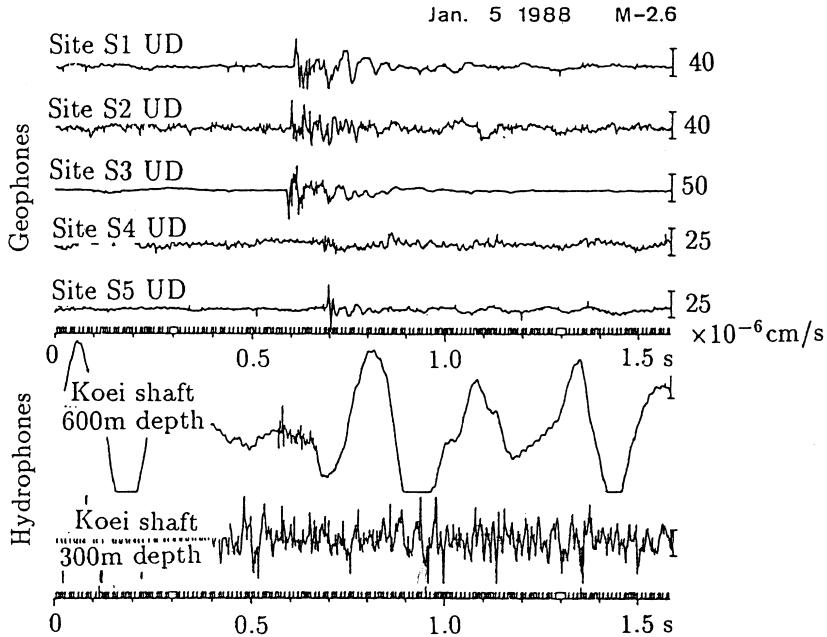


Figure 8

Examples of seismograms ( $M = -2.6$ ). Refer to Fig. 3(d) for the instrument configuration.

station corrections and by the hydrophones are shown by circles in Figs. 3(a–c), with all events in locations relevant to the present study. With respect to these, the hypocenters determined only from station corrections and geophones (the squares in Figs. 3(a–c)) do not differ by several tens of meters. Consequently, a homogeneous structure is a reasonable velocity model with acceptable accuracy for locations in this study if we take into account the station corrections. Since only four events occurred during hydrophone operation, most events were located using only geophone data and station corrections. The magnitude was determined using maximum velocity amplitude according to the empirical relationship of WATANABE (1971).

#### *b) Relationship Between Seismic Events and Geology*

A total of 56 events were detected in the Ikuno mine over a five-year period (Fig. 5(a)), the largest one about  $M = 0$ . It is important to note that all events occurred in the Kanagase area within deep ore veins (Fig. 9), while no seismic events occurred within shallow ore veins in other areas, such as Tasei or Aokusa (Fig. 2).

Seismicity in the Kanagase area can be characterized as follows:

- (1) The area with the deepest ore veins, between the Nendo and Nii faults (NeF and NiF in Fig. 9(a)), is the most active.

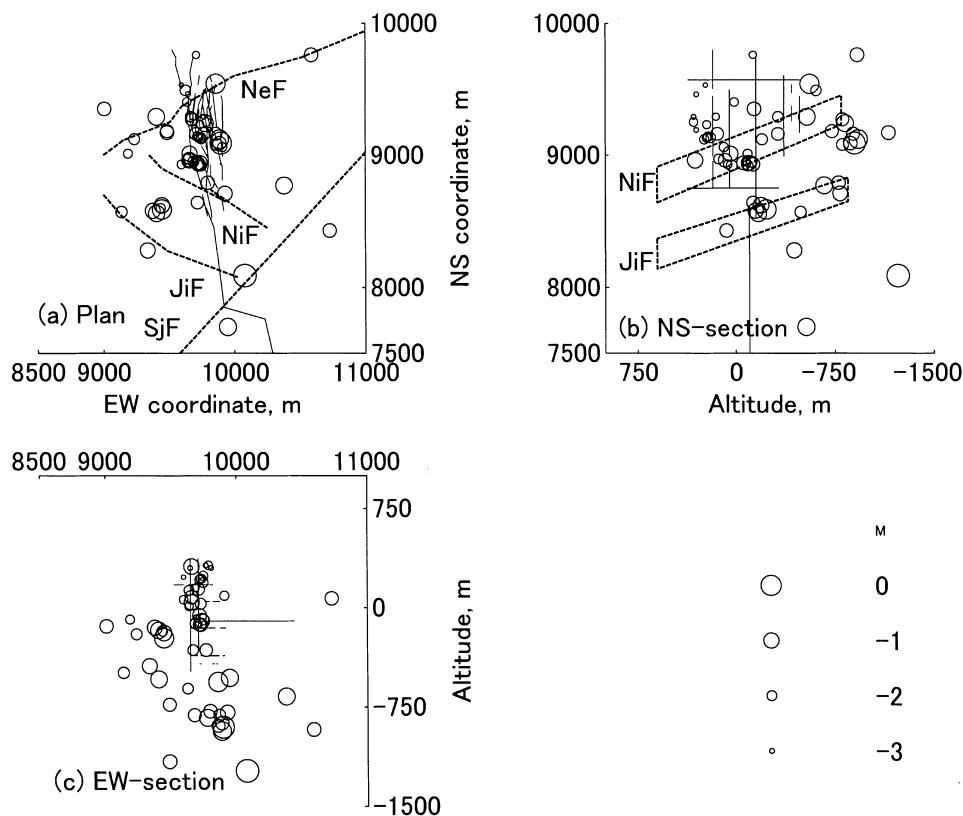


Figure 9

Relationship between hypocenters (o), faults (thick, dashed lines) and flooded tunnels through major ore veins (thin veins). NeF: Nendo fault, NiF: Nii fault, JiF: Juichii fault, SjF: Sanjugo fault. (a): Plan view of epicenters and surface traces of faults. (b) and (c): Hypocenters projected on N-S cross section and an E-W cross section, respectively.

- (2) The highest activities occur at an altitude of about 0 m, where the Nii and Juichii faults offset the ore veins (see NiF and JiF in NS-section; Fig. 9(b)).
- (3) The events occur at an altitude of about -750 m, substantially deeper than the excavated veins and near the faults (Fig. 9(b));
- (4) Seismicity occurs around the upper edge of a vertical ore vein, although it consists of small events (Figs. 9(b and c));
- (5) Activity can be observed along the Nendo fault (Fig. 9(a)).

### c) Composite Focal Mechanism

Figure 10 displays the composite focal mechanism of all 56 seismic events shown in Figure 9. In the case of distant hypocenters in layered structures with significant differences in velocity, direct arrivals will generally depart downward from sources,

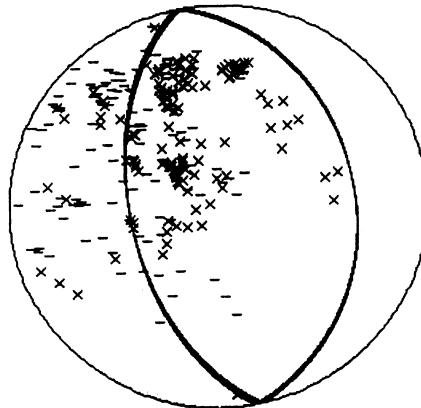


Figure 10

Composite focal mechanism for events in the Kanagase area. The composite pattern of initial push-pull of the  $P$  wave for all events detected over a 5-year period is represented by '+' and '−', respectively, on the upper hemisphere of the Wolf net. We assumed that direct arrivals departed from sources upward because the geophone arrays were deployed on underground intact rock and velocity seems not to dependent on depth. The mechanism is not for a single event, therefore the nodal planes are drawn so as to maximize the difference between the number of cases of push and pull.

and an inappropriately assumed source depth or take-off angles could lead to misunderstandings of the focal mechanism. However, the scope of our interest can be regarded as primarily a homogeneous velocity structure; our geophone array is deployed in underground intact rock, and hypocenters are near and below our array. We therefore assumed that all direct arrivals departed sources in an upward direction and came straight toward our array.

Figure 10 indicates thrust faulting consistent with the nearly horizontal E-W compressive tectonic stress state (TANAKA *et al.*, 1989). Different mechanisms may be present in the composite mechanism and we can only observe the average stress state that induces seismicity. Nonetheless, the E-W compression is inconsistent with many events which occur around the upper edge of the vertical cavity, if we assume the opening of a vertical cavity as a cause of seismicity. This is because an E-W tensile stress state is expected around the edge of the cavity, as inferred from Figure 7. Consequently, we suggest that elastic response cannot account for the composite mechanism.

#### *d) Correlation of Seismicity with the Amount of Heavy Rainfall*

Figure 5(a) shows the magnitude of each event plotted against time. The horizontal lines in Figure 5(a) represent periods with no available data. Although the periods without data are not short, the correspondence of seismicity to the rise in the water table Figure 5(f) can be seen *prima facie*. However, the seismicity

corresponds imprecisely to the water level, since event frequency does not always peak when the water level peaks. The frequency increases with some delay from the onset of heavy rainfall, or the peak water level, and the event frequency will continue to be high even after any significant changes in water and strain have ceased. This clearly shows that the elastic response of the ground to the water load is not directly responsible for the seismicity.

Figure 5(b) shows the cumulative seismic moment versus time. The seismic moments were calculated from magnitudes according to the magnitude-moment relationship of HANKS and KANAMORI (1979). As can be seen in Figure 5(b), larger events appear to occur associated with heavy rainfall, although with significant delay.

Figure 11 represents the hypocenter distribution with diamonds scaled by time lapse since the onset of heavy rainfall. Interestingly, all the events within a few

Figure 11 consists of three maps labeled (a), (b), and (c). Map (a) is a plan view with the NS coordinate (m) on the vertical axis (ranging from 7500 to 10000) and the EW coordinate (m) on the horizontal axis (ranging from 8500 to 11000). It shows several diamond-shaped hypocenters clustered around a central point, with dashed lines labeled NeF, NiF, JiF, and SjF indicating fault zones. Map (b) is an NS-section with the Altitude (m) on the vertical axis (ranging from 7500 to 10000) and the NS coordinate (m) on the horizontal axis (ranging from 750 to -1500). It shows diamond-shaped hypocenters distributed along a fault line, with dashed lines labeled NeF, NiF, and JiF. Map (c) is an EW-section with the Altitude (m) on the vertical axis (ranging from -1500 to 750) and the EW coordinate (m) on the horizontal axis (ranging from 8500 to 11000). It shows diamond-shaped hypocenters clustered around a central point. A legend on the right side of map (c) provides a key for the delay in days:

Symbol	Delay in day
Small diamond	160
Large diamond	80
Diamond with cross-hatch	40
Large open diamond	< 20

Figure 11

Relationship between the delay in time after heavy rainfalls and the location and depth of seismicity. Diamonds: hypocenters scaled by the delay of the seismic event compared to the time of heavy rainfall. Dashed line: faults, thin line: flooded tunnels near ore veins. NeF, NiF, JiF and SjF: Nendo, Nii, Juichii and Sanjugo faults, respectively.

months after the heavy rainfall occurred near the faults that offset the deepest ore veins, whereas all those located away from the deepest ore veins took place many months after the heavy rainfall. The shallower the hypocenters, the faster the response. Consequently, it is strongly suggested that diffusion controls the occurrence of the events.

### *6. Conclusions*

Fifty-six microearthquakes recorded over a 5-year period were located around the mined and flooded, vertical ore veins that extend to 1 km deep (Figs. 2, 5(a), 9 and 11). During this 5-year period, heavy rainfalls of several tens of millimeters elevated the water table several times and flooded the vertical ore veins to a depth of several meters (Figs. 5 (c) and (f)). Significant changes in strain and tilt larger than  $10^{-6}$  (Fig. 5(g)) were also monitored at the crustal movement monitoring station located several hundred meters from the veins. By simply multiplying strains larger than about  $2 \times 10^{-6}$  by an elastic modulus of about 50 GPa, the strain changes corresponded to stress changes of about 0.1 MPa. We infer that the opening of the deep tabular cavities led directly to the significant strain and tilt we observed (Fig. 3 and Table 2), but not directly to the seismicity, for the following reasons:

(1) The seismicity seemed to respond to water level elevation as well as to strain and tilt, although the delay in the seismicity was significant, and the seismicity tends to persist even after the change in strain and tilt had ceased.

(2) After more-efficient drain pumps were introduced, the seismicity seemed to respond to heavy rainfall, even though elevation of the water table did not take place.

(3) Associated with heavy rainfalls, the moderate and slow changes in strain and tilt corresponding to a stress change of 0.1 MPa ( $= 2 \times 10^{-6} \times 50$  GPa) persisted for several months, suggesting the diffusion of water underground.

(4) Some seismic events had focal mechanisms inconsistent with the stress state expected from the opening of a vertical tabular cavity.

The faults in the Ikuno mine have preferred orientations in accord with seismic events in the present stress state; direct elastic response to the load or water pressure was significant and larger than 0.1 MPa. However, this direct rise in pressure did not stimulate seismicity around the faults in the Ikuno mine, probably because the faults were not optimally oriented with respect to the stress increase. Consequently, the localized and delayed diffusion of water played the dominant role in stimulating seismicity in the Ikuno mine, though the change in pore pressure was slow and decidedly less significant than the direct change in stress due to an increase in the water load.

### Acknowledgments

We express our sincere thanks to Mitsubishi Material Co. Ltd., Silver Ikuno Co. Ltd. and Techno Ohte Co. Ltd., who kindly gave us permission to carry out our multidisciplinary observations in the closed mine and assisted in the continuation of the observations. We are grateful to Mrs. S. Ogata and H. Matsumoto of Techno Ohte Co. Ltd., who kindly supplied us with water table data for the Koei shaft and assisted us in carrying observations. We are grateful to Mr. S. Kotani of Mitsubishi Material Co. Ltd. and to colleagues at Kyoto University, who have helped us to conduct the multidisciplinary observations.

Lastly, we thank Dr. C. Trifu and two anonymous reviewers for their kind and valuable suggestions for improving our manuscript.

### REFERENCES

- EVANS, D. M. (1966), *Man-made Earthquakes in Denver*, Geotimes 10, 11–17.
- FLETCHER, J. B. and SYKES, J. R. (1977), *Earthquakes Related to Hydraulic Mining and Natural Seismic Activity in Western New York State*, J. Geophys. Res. 82, 3767–3780.
- HANKS, T. C. and KANAMORI, H. (1979), *A Moment Magnitude Scale*, J. Geophys. Res. 84, 2348–2350.
- HEALY, J. H., RUBEY, W. W., GRIGGS, D. T., and RALEIGH, C. B. (1968), *The Denver Earthquakes*, Science 161, 1301–1310.
- KOYAMA, T. (1998), *An Interpretation of Tidal Change of Water Level at the Chuo Shaft at Ikuno Mine, Japan*. Master's Thesis, Graduate School of Science and Engineering, Ritsumeikan Univ. (in Japanese).
- MCGARR, A. and SIMPSON, D., *A broad look at induced and triggered seismicity*. In *Rockbursts and Seismicity in Mines* (eds Gibowicz, S. J. and Lasocki, S.) (Balkema, Rotterdam 1997) pp. 385–396.
- NISHIDA, R. and TANAKA, Y. (1972), *Ground Tremors Caused by Rock Bursts in the Ikuno Mine* (continued), Disast. Prev. Res. Inst., Kyoto Univ. 15-B, 43–51 (in Japanese with English abstract).
- OGASAWARA, H., FUJIMORI, K., KOIZUMI, N., FUJIWARA, S., NAKAO, S., NISHIGAMI, K., TANIGUCHI, K., OTSUKA, S., HIRANO, N., NISHIDA, R., and IIO, Y. (1992), *Comprehension Observatiion System at Old Ikuno Mine for Earthquake Prediction*, Ann. Dissast. Prev. Res. Inst., Kyoto Univ. 35B-1, 389–400 (in Japanese with English abstract).
- OKADA, Y. (1992), *Internal Deformation Due to Shear and Tensile Faults in a Half Space*, Bull. Seismol. Soc. Am. 82, 1018–1040.
- RALEIGH, C. B., HEALY, J. H., and BREDEHOEFT, J. D. (1976), *An Experiment in Earthquake Control at Rangeley, Colorado*, Science 191, 1230–1237.
- SIMPSON, D. W., LEITH, W. S., and SCHOLZ, C. H. (1988), *Two Types of Reservoir-induced Seismicity*, Bull. Seismol. Soc. Am. 78, 2025–2040.
- SIMPSON, D. W. and NEGAMATULLAEV, S. Kh. (1981), *Induced Seismicity at Nurek Reservoir*, Bull. Seismol. Soc. Am. 71, 1561–1586.
- TABEI, T., FUJIMORI, K., and TANAKA, Y. (1985), *Observation of Crustal Movements at Ikuno (1977–1983)*, J. Geod. Soc. Jpn. 31, 189–201 (in Japanese with English abstract).
- TANAKA, Y. and NISHIDA, R. (1971), *Ground Tremors Caused by Rock Bursts in the Ikuno Mine*, Bull. Disast. Prev. Res. Inst., Kyoto Univ. 14-A, 149–164 (in Japanese with English abstract).
- TANAKA, Y. and NISHIDA, R. (1977), *Generation mechanism of rock bursts and microearthquakes induced by water-injection into a deep abandoned mine*, Proc. 5th Jpn. Symp. Rock Mech. 91–96 (in Japanese).
- TANAKA, Y. and OKA, Y. (1979), *Generation Mechanism of Rock Bursts and Water-induced Earthquakes under the Tectonic Stress Field*, Rock Mech. Jpn. 3, 71–73.

- TANAKA, Y., FUJIMORI, K., and TAKEUCHI, T. (1989). *Comparison Between Measured Crustal Stress Changes and Observed Crustal Strain Changes*, Ann. Disas. Prev. Res. Inst., Kyoto Univ., 32B-1, 61–73 (in Japanese with English abstract).
- WATANABE, H. (1971). *Determination of Earthquake Magnitude at Regional Distance in and near Japan*, Zisin (J. Seismol. Soc. Jpn.), Ser. 2, 24, 189–200 (in Japanese with English abstract).
- Wetmiller, R. J., Galley, C. A. and Plouffe, M., *Post-closure seismicity at a hard rock mine*. In *Rockbursts and Seismicity in Mines 93* (ed. Young, R. P.) (Balkema, Rotterdam 1993) pp. 445–448.

(Received March 21, 2000, revised/accepted July 17, 2000)



To access this journal online:  
<http://www.birkhauser.ch>

---